New Journal of Physics
The open access journal at the forefront of physics

Deutsche Physikalische Gesellschaft DPG IOP Institute of Physics

PAPER • OPEN ACCESS

Quantum synchronization in presence of shot noise

To cite this article: Florian Höhe *et al* 2025 *New J. Phys.* **27** 023039

IOP Publishing New J. Phys. 27 (2025) 023039 https://doi.org/10.1088/1367-2630/adb777

New Journal of Physics

The open access journal at the forefront of physics

Deutsche Physikalische Gesellschaft DPG
IOP Institute of Physics

Published in partnership with: Deutsche Physikalische Gesellschaft and the Institute of Physics

CrossMark

OPEN ACCESS

RECEIVED
17 September 2024

REVISED
31 January 2025

ACCEPTED FOR PUBLICATION
18 February 2025

PUBLISHED
27 February 2025

PAPER

Quantum synchronization in presence of shot noise

Florian Höhe[1,*], **Lukas Danner**[1,2], **Ciprian Padurariu**[1], **Brecht I C Donvil**[1], **Joachim Ankerhold**[1] and **Björn Kubala**[1,2]

[1] Institute for Complex Quantum Systems and IQST, University of Ulm, 89069 Ulm, Germany
[2] German Aerospace Center (DLR), Institute of Quantum Technologies, 89081 Ulm, Germany
[*] Author to whom any correspondence should be addressed.

E-mail: florian.hoehe@uni-ulm.de

Keywords: superconducting circuits, Josephson photonics, quantum synchronization, full counting statistics, nonlinear quantum dynamics

Supplementary material for this article is available online

Abstract

Synchronization is a widespread phenomenon encountered in many natural and engineered systems with nonlinear classical dynamics. How synchronization concepts and mechanisms transfer to the quantum realm and whether features are universal or platform specific are timely questions of fundamental interest. They can be studied in superconducting electrical circuits which provide a well-established platform for nonlinear quantum dynamics. Here, we consider a Josephson-photonics device, where a dc-biased Josephson junction creates (non-classical) light in a microwave cavity. The combined quantum compound constitutes a self-sustained oscillator: a system susceptible to synchronization. This is due to the inherent effect of an in-series resistance, which realizes an autonomous feedback mechanism of the charge transport on the driving voltage. Accounting for the full counting statistics of transported charge not only yields phase diffusion, but allows us to describe phase locking to an ac-signal and the mutual synchronization of two such devices. Thereby one can observe phase stabilization leading to a sharp emission spectrum as well as unique charge transport statistics revealing shot noise induced phase slips. Two-time perturbation theory is used to obtain a reduced description of the oscillators phase dynamics in form of a Fokker–Planck equation in generalization of classical synchronization theories.

1. Introduction

Since Huygens's first study of pendulum clocks in 1665 [1] the nonlinear phenomenon of synchronization has extensively been studied in all fields of science [2–6]. It occurs in systems autonomously undergoing *self-sustained oscillations*, i.e. these are not powered by an external periodic drive, but are kept going by resupplying energy in an incoherent manner, such as by the gravity-driven weight in a pendulum clock or by a battery. In the absence of any periodic reference oscillation, self-sustained oscillations do not have any preferred phase which instead will be randomized by noise acting on the system. In the same manner, the phase will be strongly susceptible to regular external perturbations, so that even a weak injected signal can entrain one oscillator or a weak coupling can synchronize the motion of two such systems. While the oscillation spectrum of the free self-sustained oscillator is broad and centered around its natural frequency, it will be pulled towards the frequency of the injected signal and become very sharp when locked, explaining the technological relevance of locking and synchronization, e. g. in laser physics [7, 8].

Unsurprisingly, also quantum synchronization has attracted interest recently, both for systems whose classical counterparts show synchronization behavior with the paradigmatic example of the van der Pol oscillator [9–16], as well as for systems [17–25], such as small spins, or mechanisms [26–32] without classical analogue.

Superconducting electrical circuits incorporating Josephson junctions are an ideal platform to study, both, the fundamental physics of (circuit) quantum electrodynamics as well as the technological exploitation of nonlinear quantum dynamics. For instance, such circuits can oftentimes bridge all the way from the semiclassical to the deep quantum regime. One manifestation of quantum effects is the appearance of shot noise: fluctuations of the electrical current associated with the granular nature of electrical charges, i.e. of electrons in a metal or (Cooper-)pairs of electrons in a superconductor. Synchronization physics in such devices is thus influenced by the quantum mechanical nature of the nonlinear oscillator and the quantum stochastic nature of the noise affecting its phase.

A perfect system to study such quantum synchronization in the presence of shot noise are Josephson-photonics devices, where Cooper pairs (CPs) tunneling across a dc-biased Josephson junction create photons in an in-series microwave cavity [33]. In such devices, the nonlinearity of the Josephson junction imprints a quantum nature on the microwave generation so that they can be employed to create entangled light [34], photon multiplets [35], or single-photons [36, 37]. Constituting versatile and bright quantum light sources they may become an important component for quantum technological applications [38, 39] in quantum communication, quantum information processing, and for sensing and imaging tasks, such as envisioned quantum radars [40]. While synchronization in (multi-mode) Josephson photonics has been observed in a semiclassical regime [41–43] and to some extent theoretically described [44–46], those devices are also particularly suited to study the deep quantum regimes of strong nonlinearity at the few-photon level [35, 37, 47], where such fundamental questions as quantum measures of synchronization [48–50] and synchronization of individual trajectories [26, 31] can be studied.

Here, we present a model for the quantum dynamics of a Josephson-photonics circuit biased by a realistic voltage source. We show that the system is driven into self-sustained oscillations and describe how it synchronizes to an external ac-signal or a second circuit. Such phase locking enables an immediate exploitation of these devices as sources of entanglement, thus dispensing with the elaborate scheme developed in [34] to characterize the entanglement of a two-mode squeezed state without phase stability, and opens the door to Wigner state tomography consequently broadening the potential technological impact of these devices. Moreover, this new platform for quantum synchronization allows studying fundamental limitations of phase stabilization in a regime, where the quantum shot noise of charge tunneling-events feeds back into the Hamiltonian and induces phase slips.

2. Quantum synchronization to an external signal

In a Josephson-photonics device CPs tunneling across a dc-biased Josephson junction create photonic excitations in a microwave cavity connected in series with the junction, see figure 1(a). The energy of CPs is converted into microwave radiation emitted from the leaky cavity with a frequency, $\omega_J \approx 2eV_{\rm dc}/\hbar = \omega_{\rm dc}$, when the dc-voltage is tuned close to a resonance frequency, $\omega_0 \approx \omega_J$, of the cavity. Placing a resistor R_0 in series with junction and cavity promotes a back-action of the CP tunneling on the voltage driving the tunneling process: the mean dc-current $\langle \hat{I}_{\rm CP}\rangle$ reduces the effective dc-voltage driving the junction, $\omega_J = 2e(V_{\rm dc} - R_0\langle \hat{I}_{\rm CP}\rangle)/\hbar$, while current shot noise is turned into voltage fluctuations assumed here to exceed thermal or other fluctuations of the voltage source. As we demonstrate in the following, the very same backaction mechanism can help to avert broadening, if a small ac-locking signal is added to the dc-voltage, $V(t) = V_{\rm dc} + V_{\rm ac}\cos[\Omega t + \varphi_{\rm ac}]$. Increasing the amplitude $\varepsilon = 2eV_{\rm ac}/(\hbar\Omega)$, the spectrum will first show an additional small δ-peak at Ω, while the broadened peak is pulled towards Ω, until eventually most light is emitted within a very sharp peak in sync with the external locking drive, see figure 1(b). How to model and simulate these fundamental features of nonlinear quantum dynamics – namely frequency pulling, phase locking, and the closely related synchronization to a second device, which takes the role of the external locking signal – is the central result of this work.

2.1. Josephson-photonics system with in-series resistor

A Josephson-photonics device is modeled by the Hamiltonian

$$H_S = \hbar\omega_0 \hat{a}^\dagger \hat{a} - E_J \cos\left[\alpha_0\left(\hat{a}^\dagger + \hat{a}\right) + \frac{2e}{\hbar}\int_0^t V(\tau)\,\mathrm{d}\tau - \hat{\varphi}_{R_0}\right], \qquad (1)$$

where $\hat{a}^\dagger$ and $\hat{a}$ denote creation and annihilation operators of the cavity with zero-point fluctuations $\alpha_0 = (2e^2\sqrt{L/C}/\hbar)^{1/2}$, E_J is the Josephson energy, and the argument of the cosine follows from Kirchhoff's sum rule. In contrast to ac-driven Josephson microwave devices, such as Josephson parametric amplifiers [38, 39], the nonlinear Josephson-photonics device is not driven by a periodic force, but by an incoherent power input from a battery. It thus emulates the textbook dynamical system susceptible to locking and synchronization, the pendulum clock driven by a weight. This aspect of Josephson-photonics devices is hidden in the standard description, when a perfect dc-voltage bias $V \equiv V_{\rm dc}$ without any resistance is assumed, i.e. $\hat{\varphi}_{R_0} = 0$, so that a periodic drive term $E_J\cos\left[2eV_{\rm dc}t/\hbar + \alpha_0(\hat{a}^\dagger + \hat{a})\right]$ results. The oftentimes

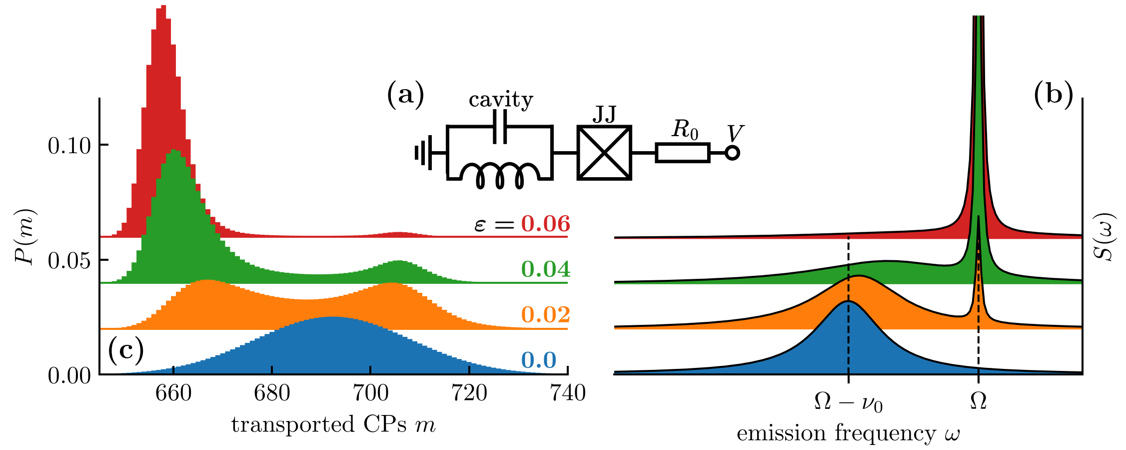

Figure 1. The microwave emission of a Josephson-photonics device (a), consisting of a Josephson junction in-series to a microwave cavity and a resistance R_0, can be locked by adding a small ac-signal (of strength ε and frequency Ω on top of a dc-voltage drive). (b) Emission spectra $S(\omega)$ are centered around a frequency ω_J determined by the voltage across the junction but broadened by phase fluctuations. Applying a locking signal [initially detuned by $\nu_0 = \Omega - \omega_J(\varepsilon = 0)$] pulls the emission frequency towards Ω, eventually resulting in a sharp emission peak at Ω [here artificially broadened by $\gamma/1000$ (FWHM)]. (c) The counting statistics of CPs transported within a time interval $T = 267/\gamma$ is directly linked to the statistics of voltage fluctuations and thus the spectral width. Increasing the locking strength narrows the CP distribution, while shot noise induces phase slips by $\Delta m = 1/r_0$. [Parameters: $E_J^*/(\hbar\gamma) = 20$, $\alpha_0 = 0.1$, $2eV_{\mathrm{dc}}/\hbar = \omega_0$, $\nu_0 = 1.25 r_0\gamma$, $r_0 = 1/50$.].

neglected fluctuations of the voltage [51] turn the system into a (lockable) self-sustained oscillator. These fluctuations arise from thermal or external sources, but crucially contain an unavoidable contribution from the shot noise of the current through the junction. We describe this by considering a resistance in-series with a perfect voltage source, as visualized in figure 1(a). The integrated voltage fluctuations due to shot noise on this resistance yield the phase,

$$\hat{\varphi}_{R_0} = (2e/\hbar)\int_0^t \hat{V}_{R_0}\mathrm{d}\tau = (2e/\hbar)\,R_0\int_0^t \hat{I}_{\mathrm{CP}}\mathrm{d}\tau\,, \tag{2}$$

appearing in (1).

In general, the current in (2) is a full quantum operator and so is the integral for the phase, which being proportional to the number of CPs m transferred across the junction in the elapsed time interval incorporates the effects of coherences between different charge transfer numbers. In a model without in-series resistance these coherences are limited by the typical number of photons in the cavity and a resistance will introduce additional decoherence. Instead of retaining the full quantum character of $\hat{\varphi}_{R_0}$ and a full microscopic model of the resistance in the Hamiltonian, we can effectively model the resistor phase by treating the number m of transferred CPs as a stochastic variable with statistics described by the full counting statistics of the coherent CP tunneling process. Such a modeling of the driving phase in the Hamiltonian (1) by an m-dependent c-number, $\varphi_{R_0} = 2\pi r_0 m$, where $r_0 = R_0/R_Q$ is the in-series resistance in units of the superconducting resistance quantum $R_Q = h/(4e^2)$, is valid for small r_0, where any residual coherences between charge states would correspond to minute changes of the driving phase. Using the m-dependent Hamiltonian (1) within a quantum master equation for the state of the system, which is conditioned on the number of tunneled CPs, resembles a feedback-based locking scheme, where the in-series resistance realizes an inherent autonomous adaptation of the driving phase to a measurement outcome.

The model outlined here comprises two essential components that extend beyond the standard description of Josephson photonic devices used in previous works. First, a small ac-voltage signal is added on top of the usual dc-bias and we need to derive the rotating-wave Hamiltonian of the system incorporating both these voltages. Second, the in-series resistance turns the system into a self-sustained oscillator and we require an equation governing the time-evolution of the system that accurately reflects the dynamics of the m-dependent parameter φ_{R_0}. These two extensions are covered in sections 2.2 and 2.3, respectively. Together, this will provide a complete model that can be simulated numerically or simplified through approximations to a reduced description of the phase.

2.2. Hamiltonian: inclusion of a small ac-voltage signal

Technically, we first move to a frame rotating with the frequency Ω of the ac-signal (introducing a detuning $\Delta = \delta_{\mathrm{dc}} + \delta_{\mathrm{ac}} = (\omega_0 - \omega_{\mathrm{dc}}) + (\omega_{\mathrm{dc}} - \Omega)$) while neglecting fast oscillating terms in a rotating wave approximation (RWA). The resulting Hamiltonian (cf appendix A), $H_{\mathrm{RWA}} = \hbar\Delta a^\dagger a + h + h^\dagger$, with

$$h^\dagger(m) = \frac{E_J^*\alpha_0}{2}\mathrm{e}^{\mathrm{i}\psi} : ia^\dagger \frac{J_1\left(2\sqrt{\alpha_0^2 a^\dagger a}\right)}{\sqrt{\alpha_0^2 a^\dagger a}} : + \varepsilon\frac{E_J^*}{4}\mathrm{e}^{\mathrm{i}\psi} : a^{\dagger 2}\frac{J_2\left(2\sqrt{\alpha_0^2 a^\dagger a}\right)}{a^\dagger a} + J_0\left(2\sqrt{\alpha_0^2 a^\dagger a}\right) :$$
$$\approx \frac{E_J^*\alpha_0}{2}\mathrm{e}^{\mathrm{i}\psi}\, ia^\dagger + \varepsilon\frac{E_J^*}{4}\mathrm{e}^{\mathrm{i}\psi}\left[\frac{\alpha_0^2 a^{\dagger 2}}{2} + \left(1 - \alpha_0^2 a^\dagger a\right)\right], \tag{3}$$

depends on the phase-difference

$$\psi(t,m) = \Omega t + \varphi_{\mathrm{ac}} - (\omega_{\mathrm{dc}} t - 2\pi r_0 m) \tag{4}$$

between the ac-signal and the cavity oscillation. Here, the Josephson energy is renormalized, $E_J^* = E_J\mathrm{e}^{-\alpha_0^2/2}$, and colons signal normal-ordering of the operators. The second line, valid for small zero-point fluctuations and weak driving, so that all Bessel functions may be expanded, allows easy interpretation of the various terms: the first term describes direct driving of the cavity by the dc-bias, where each tunneling CP creates a photon; the second term, $\propto a^{\dagger 2}\cdot E_J\cdot\varepsilon$, accounts for the generation of two photons by one CP and one ac-drive excitation; and the last term represents one CP tunneling and emitting an excitation into the drive renormalized by the presence of cavity photons (see also appendix A). The various CP transfer processes come with different leading powers of the zero-point fluctuations, α_0, and accordingly for small α_0 the first term of (3) is dominant (and the approximation leading to the second line is valid). In consequence, if ψ were to be a fixed external parameter, the photonic state of the cavity would have a trivial dependence on ψ, which essentially rotates the state space, with only minor corrections stemming from the second term. Without a locking signal, $\varepsilon = 0$, the photonic state also determines the current, which is independent of the value of ψ, as seen by invoking energy conservation and the photon loss rate, $\propto \gamma\langle a^\dagger a\rangle$ [47], or by evaluating the explicitly ψ-dependent current operator, $\hat{I}_{\mathrm{CP}} = -i2e(h^\dagger - h)/\hbar$, acting on the trivially ψ-dependent cavity state. The fact, that the current describes changes of the number of transferred CPs m and thus of ψ, then leads to a driving phase that drifts and diffuses and to the self-sustained oscillator dynamics described above, cf figure 2 (a).

Turning on an oscillating locking signal, $\varepsilon > 0$, breaks the phase symmetry of such an oscillator and is generically expected to eventually lead to a state locked to specific constant values of $\psi \mod 2\pi$. Here, the locking mechanism can be ascribed to the third CP transfer process discussed above, $\propto \varepsilon E_J\cdot(1-\alpha_0^2 a^\dagger a)$, which - while irrelevant in the Hamiltonian (3) as an energetic shift in the $\alpha_0 \to 0$ limit - yields a Shapiro-like term in the current operator and results in a ψ dependence of the expectation value of the current. In particular, the ψ-dependence of the CP transfer and thus of m in (4) can lead to locked solutions, where $\mathrm{d}\psi/\mathrm{d}t = 0$ for specific values of $\psi \mod 2\pi$.

2.3. Time-evolution: adding a feedback-mechanism

The locking mechanism relies on the feedback of the number of transferred CPs into the phase ψ appearing in the Hamiltonian (3). We can capture this physics by a slight modification of the number-resolved master equation technique [52], which is routinely used for the counting of *incoherent* processes, such as photon emission or other rate processes appearing as Lindblad terms in the time-evolution. To generalize to the counting of *coherent* CP transport processes, the density matrix, $\rho(t) = \sum_m \rho_m(t)$ (m are half-integers), is divided into components according to the number of tunneled CPs m having crossed the Josephson junction after a time t. As explained in appendix B the half-integer indexing accounts for the coherent nature of the transfer process. The components are then coupled by CP tunneling amplitudes

$$\dot{\rho}_m = \mathcal{L}_0\rho_m - \frac{i}{\hbar}[h^\dagger(m-1/2)\rho_{m-1/2} + h(m+1/2)\rho_{m+1/2}$$
$$- \rho_{m+1/2}h^\dagger(m+1/2) - \rho_{m-1/2}h(m-1/2)]. \tag{5}$$

The contribution from $\mathcal{L}_0$ which includes photon loss $\gamma\mathcal{D}[a]\rho = \gamma(a\rho a^\dagger - \{a^\dagger a, \rho\}/2)$ with rate γ

$$\mathcal{L}_0\rho_m = -i\left[\Delta a^\dagger a, \rho_m\right] + \gamma\mathcal{D}[a]\rho_m, \tag{6}$$

does not correspond to CP tunneling-events. Different components $\rho_{m\pm 1/2}$ appear in a manner completely analogous to how counting fields are added with different signs to coherent forward and backward tunneling terms [53, 54].

Since the m-dependence of $h(m)$ is periodic, there exists a natural compactification, when we chose (without loss of generality) $M = 1/r_0 \in \mathbb{N}$ and set $\rho_M = \rho_0$. This enables numerical simulations up to such a long time, that a very large number of CPs has been transported.

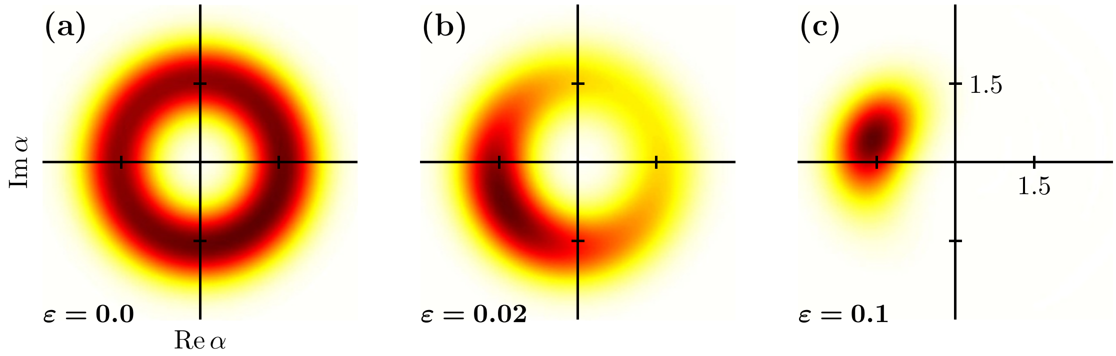

Figure 2. Wigner phase-space distributions of the cavity in the steady-state in a reference frame rotating with Ω. (a) Without locking signal the shot noise diffuses the oscillator's phase which becomes completely undefined. (c) The injection of a small ac-signal reduces the phase uncertainty, yielding a state with a sharply refocused phase in the locked regime. (b) In the intermediate regime shot noise and locking signal compete resulting in a state with partially diffused phase. [Parameters: $E_J^*/(\hbar\gamma) = 20$, $\alpha_0 = 0.1$, $2eV_{\mathrm{dc}}/\hbar = \omega_0$, $\nu_0 = 1.25r_0\gamma$, $r_0 = 1/50$. Wigner functions are normalized to their maxima.].

With this method (and the quantum regression theorem) the steady-state spectra of figure 1(b) discussed above were found. These can be compared to the counting statistics of CPs, $P(m) = \mathrm{tr}\rho_m$ after a finite time T, shown in figure 1(c). When the ac-signal is absent, the distribution of counted CPs is broad, conforming with a broad emission spectrum of the cavity. An increase of the strength of the external locking signal reduces the width in the statistics of counted CPs, pulls the frequency emission towards the locking frequency, and eventually results in a sharp photon emission spectrum and a sharpened probability distribution $P(m)$. In the long-time limit the peak of the locked distribution (red in figure 1(c)) will not become wider, but the distribution will develop many sidepeaks, see appendix B, which as we will show in the next section, are associated with slips of the phase variable by 2π.

3. Phase diffusion and its constraint by locking

The impact of the in-series resistance and resulting voltage fluctuations, and the effects of the locking signal can also be studied in a phase-space picture of the cavity dynamics. In figure 2, quantum master-equation results for the steady-state Wigner distribution are shown for different amplitudes of an injected ac-signal. The dc-voltage fixed close to resonance drives the cavity quickly into a (near coherent) state with finite amplitude. However, due to the lack of a reference phase, the imperfect dc-voltage drive across the junction disperses the neutrally stable phase of this state on the limit cycle (figure 2(a)). The resulting steady state of the system is diagonal (and hence identical in the lab and the rotating frame) and all information about the driving phase is lost. The unstable phase-space angle is mirrored by the noise-induced broadening of the emission spectrum, cf blue spectrum in figure 1(b). Turning on and progressively increasing the amplitude of the ac-voltage, the completely dephased steady-state distribution contracts and locks the state to a certain position on the limit cycle (figures 2(b) and (c)). Concomitantly the variance of the phase-space angle is reduced and a sharpened peak emerges in the emission spectrum (cf figure 1(b)). In the lab frame the state rotates with the frequency of this emission peak. Notably, in phase-space the effects of synchronization emerge completely smoothly with increasing strength ε, while the spectral pulling shows remnants of the classical criticality, see figures 1(b) and 3(c) below.

We will understand and quantify the observed dynamics of the phase-space angle by linking it to the notion of constrained diffusion. For that purpose, we again turn to the phase difference ψ between the phase of the locking signal and the phase which drives the cavity (4). The synchronized state will then be characterized by the phase difference ψ becoming constant in time (modulo 2π), as the cavity emits photons with frequencies centered sharply about the injection frequency Ω.

4. Reduced dynamics of the phase

The question that now arises is, whether a reduced equation for the dynamics of the phase variable ψ can be derived in the quantum domain, thus generalizing the Adler-theory of classical synchronization dynamics [2, 45, 55]. Indeed, the quantum master equation (5) can be rewritten as an equation for a density $\rho'(t,\psi)$ by first treating m as continuous and transforming to a moving frame as shown in appendix C. Crucially, the explicit time dependence of the Hamiltonian (3) is removed by the latter step. Assuming a time scale separation between the (fast) adaptation of the cavity state to the phase of its driving term and the slow

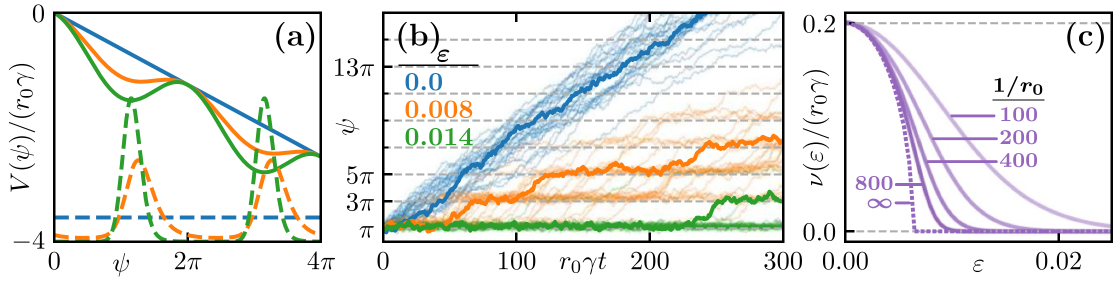

Figure 3. Dynamics of the reduced phase in a tilted washboard potential. (a) The injection of a sufficiently strong ac-signal creates a potential with minima in which periodic steady-state distributions (dashed) are found. (b) Individual trajectories of a phase particle in the potentials of (a). Long intervals of constant phase in the synchronized state (green) are interrupted by phase slips of 2π, which proliferate (orange) and overlap (blue) in the unsynchronized regime. (c) The steady-states of (a) yield the rate $\nu(\varepsilon) = \langle\dot{\psi}\rangle$ of these slips. For smaller resistance the locking transition becomes more pronounced until for $1/r_0 \to \infty$ the criticality of classical synchronization is recovered. [Parameters: $E_J^*/(\hbar\gamma) = 10$, $\alpha_0 = 0.1$, $2eV_{dc}/\hbar = \omega_0$, $\nu_0 = 0.2 r_0\gamma$, $r_0 = 1/300$.].

dynamics of the phase ψ, two-time perturbation theory can provide a Fokker–Planck equation for the dynamics on slow time scales $r_0 t$ ($r_0 \ll 1$) of the phase distribution probability [56, 57]

$$\frac{\partial}{\partial t} P(t,\psi) = -\frac{\partial}{\partial \psi}\left[j(\psi)\, P(t,\psi)\right] + \frac{\partial^2}{\partial \psi^2}\left[D(\psi)\, P(t,\psi)\right]. \quad (7)$$

The drift coefficient, in the first order of r_0, is given by $j(\psi) = 2\pi r_0 \langle \hat{I}_{CP}/(2e)\rangle - \delta_{ac}$ as derived in appendix C. In second order one obtains a correction for the drift and a diffusion term which are calculated via the pseudo-inverse of the system's Liouvillian. Without locking signal we find free diffusion of the phase with diffusion constant, $D = (2\pi r_0)^2 S_{CP}/2$, determined by the zero-frequency CP shot noise power S_{CP}. Injecting the ac-signal creates a potential $V(\psi) = -\int j(\psi)\, d\psi$ for the phase, which develops local minima for sufficient locking strength, restricting diffusion and stabilizing the phase, see figure 3(a). For small α_0 the potential simplifies to a Shapiro-like tilted washboard $V(\psi) = \nu_c \cos\psi - \nu_0\psi$ with $\nu_c = \pi r_0 \varepsilon E_J^*/\hbar$. The diffusion D remains roughly constant in this regime.

The dynamics of a phase particle in this potential is obtained via the Langevin equation corresponding to (7), see figure 3(b). Deep in the synchronized state (green), plateaus of nearly constant phase appear, interrupted by rare slips of the phase by 2π. Here, the dynamics may be approximated as an escape process which yields for $\alpha_0 \ll 1$ a Kramer's rate $\nu_K = \sqrt{\nu_c^2 - \nu_0^2}\exp\{-\Delta V/[(2\pi r_0)^2 S_{CP}/2]\}$ with $\Delta V = 2\sqrt{\nu_c^2 - \nu_0^2} + 2\nu_0 \arcsin(\nu_0/\nu_c) - \pi\nu_0$ [58]. Reducing the strength of the locking drive (orange) accordingly increases the number of slips until the synchronized plateaus are completely absent (blue). How well a system is synchronized, can be quantified by the rate of such slips. From the steady-state distributions for the phase ψ, dashed in figure 3(a), we obtain the rate of phase slips, i.e. the mean flow $\langle\dot{\psi}\rangle = \int P(\psi) j(\psi) d\psi$ in figure 3(c). For large R_0, the dependence of the phase-slip rate on the locking strength in figure 3(c) shows a shot noise induced broadening of the locking transition while in the limit $R_Q/R_0 \to \infty$ shot noise becomes negligible. Then, the Fokker–Planck equation simplifies to the well-known Adler-equation describing the locking dynamics of a classical phase variable, $\dot{\psi} = \nu_0 + \nu_c \sin(\psi)$[45].

5. Synchronization of two quantum microwave cavities

Instead of the synchronization of a single nonlinearly driven microwave cavity to an external locking signal investigated above, one can also consider the mutual synchronization of several devices [2, 59]. Dispensing with the need of a phase-stable ac-signal, the prospect of mutual synchronization of a potentially large number of devices promises a source of correlated high-intensity emission. The Hamiltonian,

$$H = H_a + H_b + \epsilon\left(a^\dagger b + a b^\dagger\right), \quad (8)$$

where

$$H_\xi = \hbar\omega_0 \xi^\dagger\xi - E_J \cos\left[\alpha_0\left(\xi^\dagger + \xi\right) + \omega_{dc,\xi} t - 2\pi r_0 m_\xi\right] \quad (9)$$

describes a scenario (see figure 4(a)), where each device $\xi = a, b$ is biased by a dc-voltage $V_\xi = \hbar\omega_{dc,\xi}/(2e)$ applied across a resistance R_0, and the coupling term stems from a small coupling capacitor and a rotating wave approximation. We assume identical devices except for differing dc-voltage drives. As before each

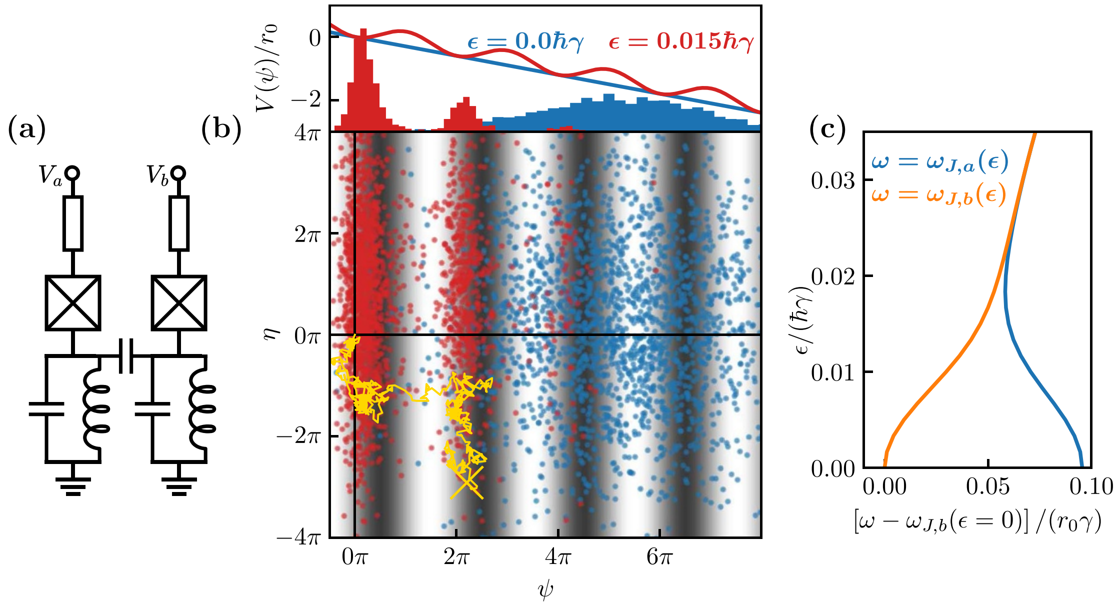

Figure 4. Statistics $P(\eta.\psi)$ of the phase-sum and -difference of two Josephson-photonics systems (a). (b) The background color indicates the force on the phase-particle in positive (white) and negative (black) ψ-direction respectively which yields the red potential shown in the panel above. The simulation shows the endpoints of individual trajectories, initially starting at $\eta = \psi = 0$, after a time $T = 170/(r_0\gamma)$ (one full trajectory is highlighted in yellow with cross at the endpoint). When the oscillators are uncoupled (blue), the phase diffuses freely in both directions. In the synchronized state (red), the phase diffuses freely along η, while the potential restricts diffusion in ψ, resulting in the emergence of two sidebands that indicate phase slips of 2π. Synchronization can be quantified by the maximum of the phase difference in phase-space $S = 2\pi \max P(\phi)$ [28], e.g. $S(\epsilon = 0.015\hbar\gamma) = 0.78$. (c) Pulling curve of the effective driving frequencies ω_J coinciding with the respective main emission peaks. [Parameters: $E_J^*/(\hbar\gamma) = 8$, $\alpha_0 = 0.1$, $2eV_a/\hbar = \omega_0$, $2e(V_a - V_b)/\hbar = 0.1 r_0\gamma$, $r_0 = 1/300$, 2000 trajectories.].

device is a self-sustained oscillator subjected to phase-diffusion on its own limit cycle. However, when two oscillators synchronize with each other, their relative phase becomes constant and stable against noise. Instead of using the driving phases of each individual oscillator as phase variables, it is therefore useful to introduce sum and difference variables

$$\eta = -2\pi r_0 \left[(m_a + m_b) - \langle m_a + m_b \rangle_{\epsilon=0}\right] \tag{10}$$

$$\psi = (\omega_{\mathrm{dc},a} - \omega_{\mathrm{dc},b})\, t - 2\pi r_0 (m_a - m_b)\,, \tag{11}$$

so that $\langle \eta \rangle_{\epsilon=0} = 0$ and $\langle \psi \rangle_{\epsilon=0}$ drifts with the effective detuning in the uncoupled case.

We again derive a 2d-Fokker–Planck equation for $P(\eta, \psi)$ by using time-scale separation, see appendix D. When the systems are uncoupled, the phase particle described by its 2d-position $\vec{x} = (\eta, \psi)$ diffuses freely, as illustrated by the statistics in figure 4. If the initially detuned oscillators are coupled ($\epsilon > 0$) one device will provide a reference frequency $\omega_{J,a}$ for the second device, which pulls the emission frequency of the second cavity $\omega_{J,b}$ towards that reference frequency, and vice versa. In the initially flat potential $V(\eta, \psi)$, minima form along the ψ direction and in the synchronized state both cavities will emit photons about the same frequency, such that $\langle \dot{\psi} \rangle \approx 0$. Hence, the statistics of the phase difference ψ becomes sharp. However, shot noise permits the phase difference to slip by 2π. Notably, the resulting strong correlation between the cavities is not associated with concomitant entanglement.

6. Context and conclusion

We compare our work to other concepts of quantum synchronization presented in the literature. One possible approach involves examining systems, that inherently exhibit distinctly quantum mechanical behavior. These include systems without classical analog like spins [60], nonlinear systems that yield negative Wigner densities [61], or systems where quantum mechanical uncertainty plays a role [48]. While our model provides a quantum description where large zero-point fluctuations quantitatively influence the synchronization behavior, its primary quantum feature is the granularity of charges which yields shot noise in the phase of the drive. This contrasts with other schemes for quantum self-sustained oscillators, where the incoherent drive is realized by a Lindblad operator with negative damping rate (van der Pol model).

Furthermore, in our approach, the Josephson photonics device achieves synchronization in a steady-state, in contrast to quantum systems that synchronize during their transient evolution [62, 63].

Instead of focusing on the quantum properties of the oscillators themselves, one can also investigate how the synchronization mechanism and the type of coupling influence synchronization dynamics in the quantum regime. Examples are measurement-induced synchronization [31], nonreciprocal couplings [64], or nonlinearly driven time crystals [65]. These differ from our work, where we consider only linear drive and coupling.

Regarding mutual synchronization there are works that directly relate synchronization to quantum correlations [66, 67] or focus on the complete equalization of the quantum states of two systems [68]. Our scenario differs from both concepts, since we focus on the regime where a description of φ_{R_0} as a c-number is sufficient: quantum correlations or entanglement are not crucial for the synchronization mechanism and the two systems only adapt their oscillation frequencies rather than their full quantum states.

To conclude, this paper introduces dc-driven Josephson-photonics devices as a new platform to study quantum synchronization in the presence of shot noise and the thereby induced phase-slip dynamics. Mechanism and modeling of quantum synchronization dynamics in such devices differ from heretofore investigated systems and do not map to the paradigmatic case of a van der Pol oscillator. Nonetheless, the system can be reduced to its phase dynamics governed by a Fokker–Planck equation with a generalized Adler potential. Implementing synchronization in Josephson-photonics devices is of technological interest due their versatility as a source of quantum microwave light, but also promises fundamental insights in a deep quantum regime, where the nature of phase slips and the potential coexistence and interplay of charge and phase tunneling [69] can be studied.

Data availability statement

The data cannot be made publicly available upon publication because they are not available in a format that is sufficiently accessible or reusable by other researchers. The data that support the findings of this study are available upon reasonable request from the authors.

Acknowledgments

We thank Andrew Armour, Julien Basset, Jérôme Estève, Benjamin Huard, and Ambroise Peugeot for fruitful discussions and acknowledge the support of the DFG through AN336/17-1 and AN336/18-1 and the BMBF through QSens (project QComp).

Appendix A. Hamiltonian in rotating wave approximation

The Hamiltonian of the dc-biased Josephson-photonics device with in-series resistance R_0 and an applied voltage $V = V_{\rm dc} + V_{\rm ac}\cos(\phi_{\rm ac})$ (where $\phi_{\rm ac} = \Omega t + \varphi_{\rm ac}$ is the phase of the ac-signal) can be derived from Kirchhoff's laws as

$$H = \hbar\omega_0 a^\dagger a - E_J \cos\left[\omega_{\rm dc} t - \varphi_{R_0} + \alpha_0\left(a^\dagger + a\right) + \varepsilon\sin\left(\phi_{\rm ac}\right)\right], \tag{A.1}$$

where $\phi_a = \omega_{\rm dc} t - \varphi_{R_0}$ (with $\omega_{\rm dc} = 2eV_{\rm dc}/\hbar$) is the driving phase of the cavity, and $\varepsilon = 2eV_{\rm ac}/(\hbar\Omega)$ is the amplitude of the ac-signal assumed to be small. We move to a reference frame rotating at $\omega_{\rm rf} \approx \omega_{\rm dc}$ with the unitary operator $U = \mathrm{e}^{\mathrm{i}\phi_{\rm rf} a^\dagger a}$, where $\phi_{\rm rf} = \omega_{\rm rf} t + \phi_0$. The Hamiltonian is then transformed as $H_{\rm rf} = UHU^\dagger + i\hbar\dot{U}U$. Linearizing the expression in the strength of the ac-signal ε, we find $H_{\rm rf} = H_0 + h + h^\dagger$ with $H_0 = \hbar(\omega_0 - \omega_{\rm rf})a^\dagger a$ and

$$h = -\frac{E_J \mathrm{e}^{-\alpha_0^2/2}}{2}\left\{\left[1 + i\varepsilon\sin\left(\phi_{\rm ac}\right)\right]\mathrm{e}^{\mathrm{i}\phi_a}\cdot \mathrm{e}^{\mathrm{i}\alpha_0 a^\dagger\cdot\exp(i\phi_{\rm rf})}\cdot \mathrm{e}^{-\mathrm{i}\alpha_0 a\cdot\exp(-i\phi_{\rm rf})}\right\}, \tag{A.2}$$

where the Josephson energy is renormalized, $E_J^* = E_J \mathrm{e}^{-\alpha_0^2/2}$. Finally, we perform a rotating wave approximation, keeping slowly oscillating terms only, resulting in

$$\begin{aligned} h \approx & -\frac{E_J^*\alpha_0}{2} i\mathrm{e}^{-\mathrm{i}[\phi_{\rm rf}-\phi_a]} : a\frac{J_1\left(2\sqrt{\alpha_0^2 a^\dagger a}\right)}{\sqrt{\alpha_0^2 a^\dagger a}} : \\ & + \varepsilon\frac{E_J^*\alpha_0^2}{8}\mathrm{e}^{-\mathrm{i}[2\phi_{\rm rf}-\phi_{\rm ac}-\phi_a]} : a^2\frac{2\cdot J_2\left(2\sqrt{\alpha_0^2 a^\dagger a}\right)}{\sqrt{\alpha_0^2 a^\dagger a}^2} + \varepsilon\frac{E_J^*}{4}\mathrm{e}^{-\mathrm{i}[\phi_{\rm ac}-\phi_a]} J_0\left(2\alpha\sqrt{a^\dagger a}\right) :, \end{aligned} \tag{A.3}$$

where each infinite series of powers of the annihilation and creation operators was written compactly as normally-ordered Bessel-functions. After defining the Adler phase ψ as the phase difference between ac-driving phase and the phase of the cavity $\psi = \phi_{\mathrm{ac}} - \phi_a$ and choosing the rotating frame such that $\phi_{\mathrm{rf}} = \phi_{\mathrm{ac}}$, we find the Hamiltonian (3) from the main text.

Appendix B. Coherent Cooper pair (CP) counting

The tunneling of CPs, the process we want to count, appears as part of the coherent time-evolution of the system, i.e. in the Hamiltonian dynamics contribution to the quantum master equation for the density matrix. This contrasts with counting emitted photons or any other incoherent process where there is a single, clear procedure to count: by introducing a counting field in a prefactor $\mathrm{e}^{\mathrm{i}\chi}$ of the photon jump operator of the Lindblad Master equation to get a generating function from the χ-dependence of the density matrix [53, 70], or fully equivalently by working in the corresponding Fourier domain by 'number-resolving' the density matrix into components corresponding to a certain number of emitted photons, whose dynamic equations are coupled by photon jumps [52].

Counting is more subtle for coherent processes. In fact, there are various schemes of introducing a counting field to the Hamiltonian part of the dynamics, which have been linked to different (virtual) measurement devices and protocols [71]. Here, we start by attaching $e^{\pm i\chi/2}$ prefactors to all terms in the Hamiltonian corresponding to the forward/backward transfer of a CP. That Hamiltonian acts from the left side on the density matrix in the coherent part of the time-evolution corresponding to the forward branch of a Keldysh contour [53], while acting from the right and residing on the backward branch, $\chi \to -\bar{\chi}$ is used. For Josephson-photonics setups where each CP transfer goes along with the creation of a cavity photon (i.e. purely dc-driven biasing without an ac-component) this method (with $\bar{\chi} \equiv \chi$) has been shown [54] to yield a coherent counting statistics identical to the incoherent photon emission statistics in the long-time limit.

To capture the effect of transferred charges on the voltage drop at the in-series resistance, namely by the driving phase's dependence on the number of charges, $\varphi_{R_0} = 2\pi r_0$, one has to go from χ-space to number space. The number-resolved quantum master equation (5) introduced in the main text corresponds to Fourier-transforming with respect to the sum variable, $\chi + \bar{\chi}$ while summing over the different numbers of transferred charges on both Keldysh branches, so that both, density matrices diagonal in the Keldysh counts (dubbed 'classical' in [72]) and off-diagonal ones contribute to the ρ_m, $2m \in \mathbb{Z}$. The average of transfers on upper and lower branch determines the fed-back charge affecting the driving phase. The off-diagonal contributions have been associated via a picture of interfering paths with negativities making $P(m) = \mathrm{tr}\rho_m$ a quasiprobability at short times which, however, do not matter due to the time-scale separation. It can easily be confirmed, that without the feedback mechanism, i.e. taking $r_0 \to 0$, the unresolved quantum master equation is found by re-summing and that the Fokker–Planck equation derived from the generalized number-resolved quantum master equation (5) yields the expected current-noise.

The *frequency-dependent current noise*

$$S_{\mathrm{CP}}(\omega) = 2\mathrm{Re}\int_0^\infty \mathrm{d}\tau \langle \delta I(t+\tau)\,\delta I(t)\rangle \mathrm{e}^{\mathrm{i}\omega\tau} \tag{B.1}$$

in the steady-state ($t \to \infty$) with $\delta I = I_{\mathrm{CP}} - \langle I_{\mathrm{CP}}\rangle$ is calculated from the full dynamical equations (3) and (5) shown in figure B1(a). Without locking the noise is the same as for the idealized case of a fixed driving phase. Due to the nonlinearity of the Josephson-photonics system the transport is slightly sub-Poissonian [73] and the noise shows (fast) features on the scale of γ in this regime. As the ac-locking signal is switched on, the slow phase dynamics changes from free diffusion to the drift and diffusion in a periodic potential and the current-correlations show signatures of this motion as sidepeaks at a frequency $|\omega| \lesssim |\nu_0|$ (yellow), which merge and develop into a dip as the phase gets trapped in the potential's minima. The feedback of the transferred charges on the driving phase correlates current fluctuations over very long times and correspondingly suppresses the zero-frequency noise down to a value connected to the total rate of phase slips. On time scales faster than the phase dynamics, the current fluctuations remain nearly unaffected.

The zero-frequency noise is of course linked to the second cumulant of the CP counting statistics. The long-time limit of $P(m)$ shown in figure 1(c) of the main text can be more easily calculated from the reduced phase dynamics, so that $P(\psi)$ (with $\psi \in \mathbb{R}$) gained from a histogram of 2000 Langevin trajectories is shown here in figure B1(b). Without locking the full counting statistics spreads out via free phase diffusion corresponding to (near-)Poissonian CP transport events as $\langle\langle \psi \rangle\rangle \propto \langle\langle m \rangle\rangle \propto Dt$, while in the locked regime ψ is distributed in peaks around the minima of the potential and spreads very slowly between these peaks by phase-slip processes.

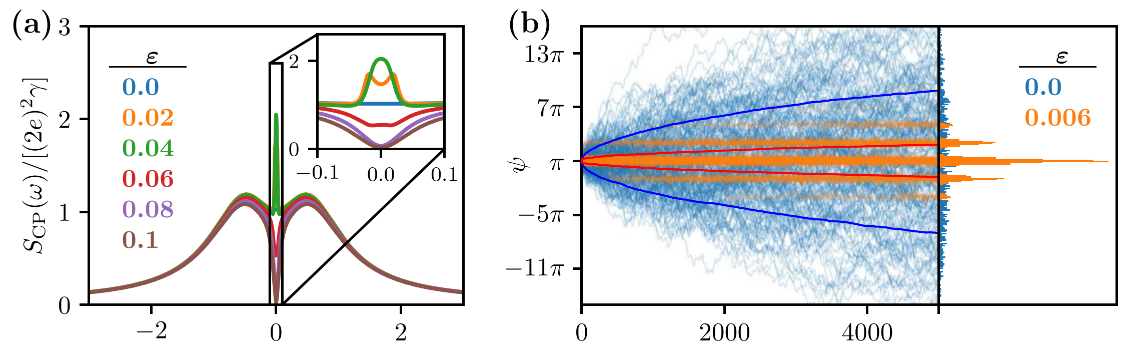

Figure B1. (a) The noise of the Cooper-pair current in a single Josephson-photonics device is analyzed for various locking amplitudes ε. At low frequencies, an injection signal initially adds noise for strengths insufficient to achieve locking, but as the system locks for larger ε, the zero-frequency noise becomes almost entirely suppressed. [Parameters see figure 1.] (b) The long-time full counting statistic of CP transport is calculated from the distribution of the phase $\psi \in \mathbb{R}$ gained from simulating 2000 trajectories. The standard deviation $\Delta\psi$ shows the $\propto \sqrt{t}$ behavior typical for diffusive processes, where the free diffusion (blue) is replaced by a much slower phase-slip process in the (weakly) locked case. [Parameters: $E_J^*/(\hbar\gamma) = 10$, $\alpha_0 = 0.1$, $2eV_{\mathrm{dc}}/\hbar = \omega_0$, $\nu_0 = 0$, $r_0 = 1/300$.].

Appendix C. Derivation of the reduced equation for the phase

Starting from the full dynamical equations we first write (5) in terms of the phase $\varphi_{R_0} = 2\pi r_0 m$ instead of the number m of transferred CP and treat φ_{R_0} as a continuous quantity $\rho_m(t) \to \rho(t, \varphi_{R_0} = 2\pi r_0 m)$. We want to express φ_{R_0} in terms of a phase ψ in a moving reference frame, which is defined by the transformation, cf (4),

$$\varphi_{R_0}(t,\psi) = \psi + \omega_{\mathrm{dc}} t - (\Omega t + \varphi_{\mathrm{ac}}). \tag{C.1}$$

Accordingly, the density matrix becomes a new function of t and ψ

$$\rho'(t,\psi) = \rho(t, \varphi_{R_0}(t,\psi)) \tag{C.2}$$

with the time derivative

$$\frac{\partial \rho'}{\partial t}(t,\psi) = \frac{\mathrm{d}\rho}{\mathrm{d}t}(t,\varphi_{R_0}(t,\psi)) = \frac{\partial \rho}{\partial t}(t,\varphi_{R_0}(t,\psi)) + \frac{\partial \rho}{\partial \varphi_{R_0}}(t,\varphi_{R_0}(t,\psi)) \frac{\partial \varphi_{R_0}}{\partial t}(t,\psi). \tag{C.3}$$

Introducing the evolution generator $\Lambda(\psi)$ this yields

$$\begin{aligned}\frac{\partial \rho'}{\partial t}(t,\psi) = \Lambda\rho'(\psi) = \delta_{\mathrm{ac}} \frac{\partial \rho'}{\partial \psi}(t,\psi) + \mathcal{L}_0 \rho'(\psi) - \frac{i}{\hbar}[h^\dagger(\psi - \pi r_0)\rho'(\psi - \pi r_0) \\ + h(\psi + \pi r_0)\rho'(\psi + \pi r_0) - \rho'(\psi + \pi r_0) h^\dagger(\psi + \pi r_0) - \rho'(\psi - \pi r_0) h(\psi - \pi r_0)]\end{aligned} \tag{C.4}$$

Note that the Hamiltonian $h(\psi) = h(t, \varphi_{R_0}(t,\psi))$ does not have an explicit time dependence, see (3).

We perform two time-scale perturbation theory (or homogenization) [74, 75] to derive an effective Fokker-Plank equation for the phase ψ. For that purpose it is assumed that the oscillator dynamics takes place on a much faster time scale than the phase dynamics. We explicitly introduce a fast time scale t and a slow time scale $\tau = r_0 t$ and the dependence of the state on these times $\rho'(t,\psi) = \rho(t,\tau,\psi)$. Then, the derivative of the density matrix becomes

$$\begin{aligned}\partial_t \rho'(t,\psi) = \frac{\mathrm{d}}{\mathrm{d}t}\rho(t,\tau,\psi) = \partial_t \rho(t,\tau,\psi) + (\partial_t \tau)\partial_\tau \rho(t,\tau,\psi) \\ = \partial_t \rho(t,\tau,\psi) + r_0 \partial_\tau \rho(t,\tau,\psi).\end{aligned} \tag{C.5}$$

Furthermore, we assume that the fast oscillator dynamics have already relaxed and we study the evolution of the state $\rho(\tau,\psi) = \lim_{t\to\infty} \rho(t,\tau,\psi)$, so that (C.4) becomes

$$r_0 \partial_\tau \rho(\tau,\psi) = \Lambda \rho(\tau,\psi) \tag{C.6}$$

In a next step, we expand $\rho(\tau,\psi) = \sum_{l=0}^{\infty} r_0^l \rho^{(l)}$ and $\Lambda\rho = \mathcal{L}\rho + r_0 \partial_\psi (\Lambda^{(1)}\rho) + \frac{1}{2} r_0^2 \partial_\psi^2 (\Lambda^{(2)}\rho) + \mathcal{O}(r_0^3)$ in orders of r_0. Taking $\rho(\psi \pm \pi r_0) = \rho \pm \pi r_0 \partial_\psi \rho + \mathcal{O}(r_0^2)$ and $h(\psi \pm \pi r_0) = h \pm \pi r_0 \partial_\psi \rho + \mathcal{O}(r_0^2)$ results in the zeroth-order Liouvillian $\mathcal{L}\rho = -\frac{i}{\hbar}[h + h^\dagger, \rho] + \mathcal{L}_0 \rho$ and for the next order $\Lambda^{(1)} = \delta_{\mathrm{ac}}/r_0 - 2\pi \mathcal{I}_{\mathrm{CP}}/(2e)$ with the symmetrized current operator $\mathcal{I}_{\mathrm{CP}}\rho = \frac{1}{2}(I_{\mathrm{CP}}\rho + \rho I_{\mathrm{CP}})$.

We proceed by solving (C.6) order by order. In *zeroth order* of r_0 we obtain

$$0 = \mathcal{L}(\psi)\rho^{(0)}(\tau,\psi) \tag{C.7}$$

which determines $\rho^{(0)}(\tau,\psi) = P^{(0)}(\tau,\psi)\rho_{\mathrm{eq}}(\psi)$ up to a factor which we interpret as a probability density $P^{(0)}(\tau,\psi)$ for a certain ψ at time τ. To find it, we consider the *first order* of $\rho(\tau,\psi)$ in r_0

$$\partial_\tau\rho^{(0)}(\tau,\psi) = \mathcal{L}(\psi)\rho^{(1)}(\tau,\psi) + \partial_\psi\left\{[\delta_{\mathrm{ac}}/r_0 - 2\pi\mathcal{I}_{\mathrm{CP}}(\psi)/(2e)]\rho^{(0)}(\tau,\psi)\right\}. \tag{C.8}$$

Taking the trace yields the desired equation of motion

$$\partial_\tau P^{(0)}(\tau,\psi) = \partial_\psi\left[\langle\delta_{\mathrm{ac}}/r_0 - 2\pi\mathcal{I}_{\mathrm{CP}}(\psi)/(2e)\rangle_{\rho_{\mathrm{eq}}(\psi)}P^{(0)}(\tau,\psi)\right] \tag{C.9}$$

which describes a drift of ψ. The *second order* (see supplemental material) in r_0 provides a correction for the drift and a diffusion term.

Then the equation of motion can be written as the Fokker–Planck equation in (7) with drift

$$j(\psi) = 2\pi r_0\langle\mathcal{I}_{\mathrm{CP}}/(2e)\rangle_{\rho_{\mathrm{eq}}(\psi)} - \delta_{\mathrm{ac}} + r_0^2\langle(\partial_\psi 2\pi\mathcal{I}_{\mathrm{CP}}/(2e)\mathcal{R})(\delta_{\mathrm{ac}}/r_0 - 2\pi\mathcal{I}_{\mathrm{CP}}/(2e))\rangle_{\rho_{\mathrm{eq}}(\psi)} \tag{C.10}$$

and diffusion

$$D(\psi) = -(2\pi r_0)^2\langle\mathcal{I}_{\mathrm{CP}}/(2e)\mathcal{R}\mathcal{I}_{\mathrm{CP}}/(2e)\rangle_{\rho_{\mathrm{eq}}(\psi)} \tag{C.11}$$

where $\mathcal{R}$ is the pseudo-inverse of $\mathcal{L}$. The r_0^2 contribution in the drift term may be neglected for small r_0.

Appendix D. Note on mutual synchronization

Two Josephson-photonics devices can be coupled, e. g. , inductively or capacitively, where we here choose to analyze a capacitive coupling. Since charge and phase are conjugate variables associated with momentum and position of the cavities, a capacitive coupling will lead to a interaction term of the form $\hat{Q}_a\hat{Q}_b \propto (a^\dagger - a)(b^\dagger - b)$ in the Hamiltonian. A sufficiently small capacitor will lead in RWA to the Hamiltonian given in the main text. We further note that a coupling capacitor modifies the eigenfrequencies of the cavities.

As in the case of locking to an ac-signal, a Fokker–Planck equation can also be derived for the synchronization of two devices. Similar to the case of injection locking, one introduces new phase variables φ_a' and φ_b' which are given by $\varphi_a' = -(\eta+\psi)/2$ and $\varphi_b = -(\eta-\psi)/2$. Calculations analogous to appendix C yield a Fokker–Planck equation for the probability density $P(t,\varphi_a,\varphi_b)$

$$\frac{\partial}{\partial t}P = \left\{-\frac{\partial}{\partial\varphi_a'}j_a - \frac{\partial}{\partial\varphi_b'}j_b + \frac{\partial^2}{\partial\varphi_a'^2}D_{aa} + 2\frac{\partial^2}{\partial\varphi_a'\partial\varphi_b'}D_{ab} + \frac{\partial^2}{\partial\varphi_b'^2}D_{bb}\right\}P \tag{D.1}$$

with drift and diffusion coefficients given in the supplemental material.

ORCID iDs

Florian Höhe https://orcid.org/0009-0008-4503-2539
Lukas Danner https://orcid.org/0000-0002-2222-2486
Ciprian Padurariu https://orcid.org/0000-0001-9568-2080
Brecht I C Donvil https://orcid.org/0000-0002-3952-6283
Joachim Ankerhold https://orcid.org/0000-0002-6510-659X
Björn Kubala https://orcid.org/0000-0001-6685-0233

References

[1] Huygens C 1897 *Oeuvres Complètes de Christiaan Huygens* vol 1 ed M Nijhoff and L Haye (Publiées par la Société hollandaise des sciences) (available at: www.biodiversitylibrary.org/bibliography/21031) pp 1888–950
[2] Pikovsky A, Rosenblum M G and Kurths J 2001 *Synchronization, A universal Concept in Nonlinear Sciences* (Cambridge University Press)
[3] Strogatz S H 2000 *Nonlinear Dynamics and Chaos: With Applications to Physics, Biology, Chemistry and Engineering* (Westview Press)
[4] Kuramoto Y 2003 *Chemical Oscillations, Waves and Turbulence* (*Dover Books on Chemistry Series*) (Dover Publications)
[5] Strogatz S H and Stewart I 1993 Coupled oscillators and biological synchronization *Sci. Am.* **269** 102–9
[6] Glass L 2001 Synchronization and rhythmic processes in physiology *Nature* **410** 277–84
[7] Buczek C J, Freiberg R J and Skolnick M L 1973 Laser injection locking *Proc. IEEE* **61** 1411–31
[8] van Tartwijk G H M and Agrawal G P 1998 Laser instabilities: a modern perspective *Prog. Quantum Electron.* **22** 43–122

[9] Walter S, Nunnenkamp A and Bruder C 2014 Quantum synchronization of a driven self-sustained oscillator *Phys. Rev. Lett.* **112** 094102

[10] Amitai E, Lörch N, Nunnenkamp A, Walter S and Bruder C 2017 Synchronization of an optomechanical system to an external drive *Phys. Rev.* A **95** 053858

[11] Walter S, Nunnenkamp A and Bruder C 2015 Quantum synchronization of two van der pol oscillators *Ann. Phys., Lpz.* **527** 131–8

[12] Lee T E and Sadeghpour H R 2013 Quantum synchronization of quantum van der pol oscillators with trapped ions *Phys. Rev. Lett.* **111** 234101

[13] Weiss T, Walter S and Marquardt F 2017 Quantum-coherent phase oscillations in synchronization *Phys. Rev.* A **95** 041802(R)

[14] Lee T E, Chan C-K and Wang S 2014 Entanglement tongue and quantum synchronization of disordered oscillators *Phys. Rev.* E **89** 022913

[15] Dutta S and Cooper N R 2019 Critical response of a quantum van der pol oscillator *Phys. Rev. Lett.* **123** 250401

[16] Arosh L B, Cross M C and Lifshitz R 2021 Quantum limit cycles and the Rayleigh and van der pol oscillators *Phys. Rev. Res.* **3** 013130

[17] Roulet A and Bruder C 2018 Synchronizing the smallest possible system *Phys. Rev. Lett.* **121** 053601

[18] Parra-López Alvaro and Bergli J 2020 Synchronization in two-level quantum systems *Phys. Rev.* A **101** 062104

[19] Koppenhöfer M, Bruder C and Roulet A 2020 Quantum synchronization on the ibm q system *Phys. Rev. Res.* **2** 023026

[20] Roulet A and Bruder C 2018 Quantum synchronization and entanglement generation *Phys. Rev. Lett.* **121** 063601

[21] Jaseem N, Hajdušek M, Vedral V, Fazio R, Kwek L-C and Vinjanampathy S 2020 Quantum synchronization in nanoscale heat engines *Phys. Rev.* E **101** 020201(R)

[22] Hush M R, Li W, Genway S, Lesanovsky I and Armour A D 2015 Spin correlations as a probe of quantum synchronization in trapped-ion phonon lasers *Phys. Rev.* A **91** 061401(R)

[23] Warsi Laskar A W, Adhikary P, Mondal S, Katiyar P, Vinjanampathy S and Ghosh S 2020 Observation of quantum phase synchronization in spin-1 atoms *Phys. Rev. Lett.* **125** 013601

[24] Krithika V R, Solanki P, Vinjanampathy S and Mahesh T S 2022 Observation of quantum phase synchronization in a nuclear-spin system *Phys. Rev.* A **105** 062206

[25] Zhang L, Wang Z, Wang Y, Zhang J, Wu Z, Jie J and Lu Y 2023 Quantum synchronization of a single trapped-ion qubit *Phys. Rev. Res.* **5** 033209

[26] Es'haqi-Sani N, Manzano G, Zambrini R and Fazio R 2020 Synchronization along quantum trajectories *Phys. Rev. Res.* **2** 023101

[27] Sonar S, Hajdušek M, Mukherjee M, Fazio R, Vedral V, Vinjanampathy S and Kwek L-C 2018 Squeezing enhances quantum synchronization *Phys. Rev. Lett.* **120** 163601

[28] Lörch N, Nigg S E, Nunnenkamp A, Tiwari R P and Bruder C 2017 Quantum synchronization blockade: energy quantization hinders synchronization of identical oscillators *Phys. Rev. Lett.* **118** 243602

[29] Nigg S E 2018 Observing quantum synchronization blockade in circuit quantum electrodynamics *Phys. Rev.* A **97** 013811

[30] Shen Y, Yi Soh H, Fan W and Kwek L-C 2023 Enhancing quantum synchronization through homodyne measurement, noise and squeezing *Phys. Rev.* E **108** 024204

[31] Schmolke F and Lutz E 2024 Measurement-induced quantum synchronization and multiplexing *Phys. Rev. Lett.* **132** 010402

[32] Kehrer T, Nadolny T and Bruder C 2024 Quantum synchronization through the interference blockade (arXiv:2405.05182)

[33] Hofheinz M, Portier F, Baudouin Q, Joyez P, Vion D, Bertet P, Roche P and Estève D 2011 Bright side of the coulomb blockade *Phys. Rev. Lett.* **106** 217005

[34] Peugeot A *et al* 2021 Generating two continuous entangled microwave beams using a dc-biased Josephson junction *Phys. Rev.* X **11** 031008

[35] Ménard G C *et al* 2022 Emission of photon multiplets by a dc-biased superconducting circuit *Phys. Rev.* X **12** 021006

[36] Grimm A *et al* 2019 Bright on-demand source of antibunched microwave photons based on inelastic cooper pair tunneling *Phys. Rev.* X **9** 021016

[37] Rolland C *et al* 2019 Antibunched photons emitted by a dc-biased Josephson junction *Phys. Rev. Lett.* **122** 186804

[38] Casariego M *et al* 2023 Propagating quantum microwaves: towards applications in communication and sensing *Quantum Sci. Technol.* **8** 023001

[39] Gu X, Frisk Kockum A, Miranowicz A, Liu Y-xi and Nori F 2017 Microwave photonics with superconducting quantum circuits *Phys. Rep.* **718** 1–102

[40] Sandbo Chang C W, Vadiraj A M, Bourassa J, Balaji B and Wilson C M 2019 Quantum-enhanced noise radar *Appl. Phys. Lett.* **114** 112601

[41] Cassidy M C, Bruno A, Rubbert S, Irfan M, Kammhuber J, Schouten R N, Akhmerov A R and Kouwenhoven L P 2017 Demonstration of an ac Josephson junction laser *Science* **355** 939–42

[42] Chen F, Li J, Armour A D, Brahimi E, Stettenheim J, Sirois A J, Simmonds R W, Blencowe M P and Rimberg A J 2014 Realization of a single-cooper-pair Josephson laser *Phys. Rev.* B **90** 020506(R)

[43] Yan C, Hassel J, Vesterinen V, Zhang J, Ikonen J, Grönberg L, Goetz J and Möttönen M 2021 A low-noise on-chip coherent microwave source *Nat. Electron.* **4** 885–92

[44] Simon S H and Cooper N R 2018 Theory of the Josephson junction laser *Phys. Rev. Lett.* **121** 027004

[45] Danner L, Padurariu C, Ankerhold J and Kubala B 2021 Injection locking and synchronization in Josephson photonics devices *Phys. Rev.* B **104** 054517

[46] Lang B, Morley G F and Armour A D 2023 Discrete time translation symmetry breaking in a Josephson junction laser *Phys. Rev.* B **107** 144509

[47] Gramich V, Kubala B, Rohrer S and Ankerhold J 2013 From Coulomb-blockade to nonlinear quantum dynamics in a superconducting circuit with a resonator *Phys. Rev. Lett.* **111** 247002

[48] Mari A, Farace A, Didier N, Giovannetti V and Fazio R 2013 Measures of quantum synchronization in continuous variable systems *Phys. Rev. Lett.* **111** 103605

[49] Ameri V, Eghbali-Arani M, Mari A, Farace A, Kheirandish F, Giovannetti V and Fazio R 2015 Mutual information as an order parameter for quantum synchronization *Phys. Rev.* A **91** 012301

[50] Shen Y, Yi Soh H, Kwek L-C and Fan W 2023 Fisher information as general metrics of quantum synchronization *Entropy* **25** 1116

[51] Wang H, Blencowe M P, Armour A D and Rimberg A J 2017 Quantum dynamics of a Josephson junction driven cavity mode system in the presence of voltage bias noise *Phys. Rev.* B **96** 104503

[52] Xu C and Vavilov M G 2013 Full counting statistics of photons emitted by a double quantum dot *Phys. Rev.* B **88** 195307

[53] Novotny T 2013 Full counting statistics of electronic transport through interacting nanosystems *J. Comput. Electron.* **12** 375–87

[54] Kubala B, Ankerhold J and Armour A D 2020 Electronic and photonic counting statistics as probes of non-equilibrium quantum dynamics *New J. Phys.* **22** 023010
[55] Adler R 1946 A study of locking phenomena in oscillators *Proc. IRE* **34** 351–7
[56] Pavliotis G A and Stuart A M 2008 *Multiscale Methods: Averaging and Homogennization* 1st Edition (Springer)
[57] Bender C M and Orszag S A 1978 *Advanced Mathematical Methods for Scientists and Engineers I* (Springer)
[58] Risken H 1996 *The Fokker-Planck equation* (Springer)
[59] Kuramoto Y 1975 *International Symposium on Mathematical Problems in Theoretical Physics* (*Lecture Notes in Physics*) vol 30 p 420
[60] Reimann P, Vorndamme P and Schnack J 2023 Nonequilibration, synchronization and time crystals in isotropic Heisenberg models *Phys. Rev. Res.* **5** 043040
[61] Lörch N, Amitai E, Nunnenkamp A and Bruder C 2016 Genuine quantum signatures in synchronization of anharmonic self-oscillators *Phys. Rev. Lett.* **117** 073601
[62] Luca Giorgi G, Cabot A and Zambrini R 2019 Transient synchronization in open quantum systems *Advances in Open Systems and Fundamental Tests of Quantum Mechanics: Proc. 684 (Bad Honnef, Germany, 2–5 December 2018) (WE-Heraeus-Seminar)* (Springer) pp 73–89
[63] Siwiak-Jaszek S, Le T P and Olaya-Castro A 2020 Synchronization phase as an indicator of persistent quantum correlations between subsystems *Phys. Rev.* A **102** 032414
[64] Nadolny T, Bruder C and Brunelli M 2025 Nonreciprocal synchronization of active quantum spins *Phys. Rev.* X **15** 011010
[65] Cabot A, Luca Giorgi G and Zambrini R 2024 Nonequilibrium transition between dissipative time crystals *PRX Quantum* **5** 030325
[66] Luca Giorgi G, Galve F, Manzano G, Colet P and Zambrini R 2012 Quantum correlations and mutual synchronization *Phys. Rev.* A **85** 052101
[67] Li W, Zhang W, Li C and Song H 2017 Properties and relative measure for quantifying quantum synchronization *Phys. Rev.* E **96** 012211
[68] Czartowski J, Müller R, Życzkowski K and Braun D 2021 Perfect quantum-state synchronization *Phys. Rev.* A **104** 012410
[69] Hriscu A M and Nazarov Y V 2013 Quantum synchronization of conjugated variables in a superconducting device leads to the fundamental resistance quantization *Phys. Rev. Lett.* **110** 097002
[70] Bagrets D A and Nazarov Y V 2003 Full counting statistics of charge transfer in coulomb blockade systems *Phys. Rev.* B **67** 085316
[71] Graf G M and Lesovik G B 2010 Time ordering and counting statistics *J. Stat. Phys.* **138** 333–50
[72] Hofer P P and Clerk A A 2016 Negative full counting statistics arise from interference effects *Phys. Rev. Lett.* **116** 013603
[73] Armour A D, Kubala B and Ankerhold J 2017 Noise switching at a dynamical critical point in a cavity-conductor hybrid *Phys. Rev.* B **96** 214509
[74] Pavliotis G A and Stuart A 2008 *Multiscale Methods: Averaging and Homogenization* (*Texts in Applied Mathematics*) (Springer)
[75] Donvil B, Muratore-Ginanneschi P and Pekola J P 2019 Hybrid master equation for calorimetric measurements *Phys. Rev.* A **99** 042127